Advances in Ceramic Matrix Composites IX

Edited by
Narottam P. Bansal
J.P. Singh
Waltraud M. Kriven
Hartmut Schneider

Ceramic Transactions
Volume 153

Advances in Ceramic Matrix Composites IX

Related titles published by The American Ceramic Society

Advances in Ceramic Matrix Composites VIII (Ceramic Transactions Volume 139)
Edited by J.P. Singh, Narottam P. Bansal, and M. Singh
©2002, ISBN 1-57498-154-4

Innovative Processing and Synthesis of Ceramics, Glasses, and Composites VI (Ceramic Transactions Volume 135)
Edited by Narottam P. Bansal and J.P. Singh
©2002, ISBN 1-57498-150-1

Innovative Processing and Synthesis of Ceramics, Glasses, and Composites V (Ceramic Transactions Volume 129)
Edited by Narottam P. Bansal and J.P. Singh
©2002, ISBN 1-57498-137-4

Advances in Ceramic Matrix Composites VII (Ceramic Transactions Volume 128)
Edited by Narottam P. Bansal, J.P. Singh, and H.-T. Lin
©2001, ISBN 1-57498-136-6

Advances in Ceramic Matrix Composites VI (Ceramic Transactions Volume 124)
Edited by J.P. Singh, Narottam P. Bansal, and Ersan Ustundag
©2001, ISBN 1-57498-123-4

Innovative Processing and Synthesis of Ceramics, Glasses, and Composites IV (Ceramic Transactions Volume 115)
Edited by Narottam P. Bansal and J.P. Singh
©2000, ISBN 1-57498-111-0

Innovative Processing and Synthesis of Ceramics, Glasses, and Composites III (Ceramic Transactions Volume 108)
Edited by J.P. Singh, Narottam P. Bansal, and Koichi Niihara
©2000, ISBN 1-57498-095-5

Advances in Ceramic Matrix Composites V (Ceramic Transactions Volume 103)
Edited by Narottam P. Bansal, J.P. Singh, and Ersan Ustundag
©2000, ISBN 1-57498-089-0

Advances in Ceramic Matrix Composites IV (Ceramic Transactions Volume 96)
Edited by J.P. Singh and Narottam P. Bansal
©1999, 1-57498-059-9

Advances in Ceramic Matrix Composites III (Ceramic Transactions Volume 74)
Edited by Narottam P. Bansal and J.P. Singh
©1996, ISBN 1-57498-020-3

For information on ordering titles published by The American Ceramic Society, or to request a publications catalog, please contact our Customer Service Department at:

Customer Service Department
735 Ceramic Place
Westerville, OH 43081, USA
614-794-5890 (phone)
614-794-5892 (fax)
info@ceramics.org

Visit our on-line book catalog at www.ceramics.org.

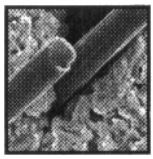

Ceramic Transactions
Volume 153

Advances in Ceramic Matrix Composites IX

Proceedings of the Ceramic Matrix Composites Symposium held at the 105th Annual Meeting of the American Ceramic Society, April 27-30, 2003, in Nashville, Tennesse.

Edited by

Narottam P. Bansal
National Aeronautics and Space Administration,
Glenn Research Center

J.P. Singh
Argonne National Laboratory

Waltraud M. Kriven
University of Illinois at Urbana-Champaign

Hartmut Schneider
German Aerospace Center, Cologne

Published by
The American Ceramic Society
735 Ceramic Place
Westerville, Ohio 43081
www.ceramics.org

Proceedings of the Ceramic Matrix Composites Symposium held at the 105th Annual Meeting of the American Ceramic Society, April 27-30, 2003, in Nashville, Tennesse.

COVER PHOTO: SEM micrograph of a potassium-based, geopolymer composite is courtesy of D.C. Comrie and W.M. Kriven and appears as figure 7 in their paper "Composite Cold Ceramic Geopolymer in a Refractory Application," which begins on page 211.

For information on ordering titles published by The American Ceramic Society, or to request a publications catalog, please call 614-794-5890.

Printed in the United States of America.

4 3 2 1–06 05 04 03

ISSN 1042-1122
ISBN 1-57498-207-9

Contents

Oxide Matrix Composites

Geopolymers and Geopolymer Matrix Composites

Mechanical Properties

Characterization

Thermal/Environmental Barrier Coatings

Preface

Advanced structural materials are needed for high-temperature applications in industries such as aerospace, power generation, and transportation. Ceramic-matrix composites are strong, tough, environmentally stable, light in weight, and have the ability to withstand high operating temperatures. This makes them viable candidate materials for high temperature structural applications.

An international symposium on recent advances in ceramic-matrix composites was held during the 105th Annual Meeting and Exposition of The American Ceramic Society, April 27–30, 2003 at the Gaylord Opryland Convention Center, Nashville, Tennessee. The objective of this symposium was to provide an international forum for scientists, engineers, and technologists to discuss and exchange ideas on state-of-the-art ceramic-matrix composites. A total of 65 papers, including invited talks, oral presentations, and posters were presented indicating continued interest in the scientifically and technologically important field of ceramic-matrix composites. Researchers from Australia, China, France, Germany, Italy, Japan, Mexico, New Zealand, South Korea, Spain, Switzerland, Taiwan, Turkey, U.K., and the United States participated. The speakers represented universities, industry, and government research laboratories.

These proceedings contain contributions on various aspects of ceramic-matrix composites that were discussed at the symposium. Twenty three papers describing the latest developments in the areas of ceramic fibers, processing and fabrication, oxide and non-oxide composites, carbon-carbon composites, geopolymer composites, mechanical behavior, corrosion and environmental effects, characterization, fiber-matrix interface, design of composites, and thermal/environmental barrier coatings, and more are included in this volume.

The editors wish to extend their gratitude and appreciation to the authors for their cooperation and contributions, to the session chairs for their time and efforts in keeping the sessions on schedule, and to the reviewers for their useful comments and suggestions. Without the contributions of all involved, this volume would not have been possible. Financial support from NASA Glenn Research Center, the Engineering Ceramics Division and The American Ceramic Society is gratefully acknowledged. Thanks are due to

the staff of the meetings and publications departments of The American Ceramic Society for their invaluable assistance.

It is our earnest hope that this volume will serve as a valuable reference for the researchers as well as the technologists in the field of ceramic-matrix composites.

Narottam P. Bansal

J. P. Singh

Waltraud M. Kriven

Hartmut Schneider

Ceramic Fibers

FINE CERAMIC FIBERS: FROM MICROSTRUCTURE TO HIGH TEMPERATURE MECHANICAL BEHAVIOR

Marie-Hélène Berger
Ecole des Mines de Paris - Centre des Matériaux
BP 87 - 91003 Evry Cedex- France
marie-helene.berger@ensmp.fr

ABSTRACT

Fine ceramic fibers used as reinforcement of structures for thermomechanical applications are reviewed. The fibers have to show sufficient flexibility, high strength and thermomechanical stability in corrosive environment. These requirements impose specific fabrication routes and a strict control of their chemistry and microstructures. The relationship between fabrication process, high temperature mechanical behavior and microstructure evolution under load is described for SiC and alumina based fibers. It is shown that fibers of close chemical compositions but differing from dopant additions exhibit distinct creep behaviors. Favorable microstructural evolutions under load controlled by appropriate intergranular chemistry are proposed to reduce creep rates. The methods used to test and charcterize fibers of 10 μm in diameter are reviewed.

INTRODUCTION

Compared to organic, glass or carbon fibers, ceramic fibers can appear as anecdotal in terms of sales volumes, however the development of advanced materials is closely bound to the availability of high performance ceramic fibers. Applications, both actual and envisaged, are for aeronautical and ground based gas turbines, combustion chambers, heat exchangers... For all of these applications the structures have to withstand very high temperatures in oxidative and corrosive environments, so excluding the use of organic-, glass- or carbon fibers. Ceramic fibers are often required to resist static or dynamic mechanical loading at high temperature, which can only be achieved by a close control of their microstructures.

Ceramic fibers have to show sufficient flexibility so that preforms can be made by weaving and subsequently infiltrated by the matrix material. Flexibility is related to $\sim E/D^3$ where E is the stiffness and D the fiber diameter. A diameter of around10 μm is therefore required if Young's modulus exceeds 300 GPa (α-Al_2O_3

or SiC fibers). A strain to failure of around 1% is also required to facilitate the weaving process. Long term chemical, microstructural and mechanical stability and creep resistance above at least 1200°C are needed. A low reactivity with matrix and interface is necessary to stop or deflect matrix cracks, which is the basis of CMC tenacity.

Alumina and silicon carbide bulk form are widely used for their high stiffness, and good high temperature mechanical properties in air. The relatively low strength of these bulk materials would be significantly increased if they could be transformed into small diameter fibers. Fine fibers must possess sub-micron grains. Moreover, for the same length, the probability of finding a critical defect in a specimen of a large cross section is much greater than in a fine fiber. The effect of any such defect will be confined to the few adjacent fibers within a composite structure. However the requirement of small diameters imposes production processes resulting in specific microstructures and properties for the fibers compared to conventional of bulk alumina and silicon carbide ceramics.

Conventional ceramic processes, which include powder compaction and sintering, cannot be extended to fine ceramic fibers. Organic or glass fibers are obtained by the spinning of a bundle from a melt of the desired final composition, a process which is precluded for fine ceramic fibers as their melting points usually exceed 2000°C. The production of fine ceramic fibers requires the spinning of an organic or mineral precursor fiber, which is then heat-treated and pyrolysed for a very short time. This process has to yield not only the desired global chemistry but also a microstructure on a scale which is much finer than the fiber diameter and remain stable at high temperature and resistant to flaws and creep. The strong relations between the fabrication processes, microstructures and macroscopic properties have to be understood and controlled if high performance fibers are to be obtained.

This paper will first present the specific test and observation methods for fine ceramic fibers and then follow the evolution in the last decades of both oxide and non-oxide ceramic fibers. The impact of small variations in the fabrication processes on the microstructure and mechanical behavior of these fibers will be reported.

FIBER TEST METHODS

Bundle tests

In order to design structures in ceramic matrix composites it is necessary to be able to quantify the strengths and creep behavior of the fibers. The failure stresses of ceramic fibers show considerable scatter so that a statistical approach is necessary to predict the failure stresses of the fibers used in structures. Bundles of several hundreds of fibers are produced. The stress distribution of the fibers can theoretically be extracted by testing the bundle directly[1,2]. Creep test of bundles is also a rapid and simple way to determine creep lifetime and to evaluate the creep rate. However in both cases testing bundles may introduce some ambiguities.

Fibers inside the bundle are not perfectly aligned and identically stretched at the beginning of the tensile test. A progressive loading of unequally stretched fibers when deformation increases is superposed to the failure of the weakest fibers and this leads to a non-linearity in the first part of the curves, Fig. 1. The progressive failure of the fibers and the redistribution of the load on the surviving fibers give to the last part of the tensile curve its dome shape. Mathematical models [1,2] enable to extract the statistical variation of the fiber strength from a bundle tensile test but this requires to know the distribution of the fiber slack. For the same reason tensile tests on bundle are not appropriate for a precise determination of the Young's modulus.

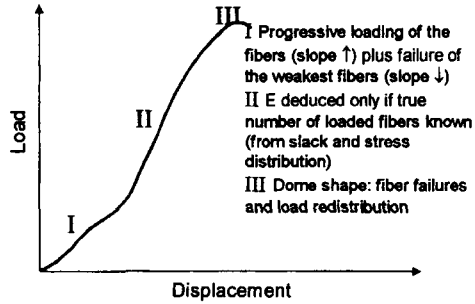

Fig. 1: Typical load vs displacement curve for tensile test on bundle.

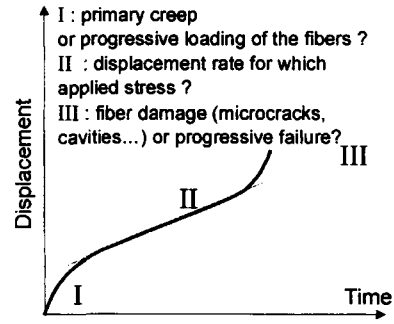

Fig. 2: Typical displacement vs time curve for creep test on bundle.

In creep experiment the decrease in the creep rate due the progressive loading of the fiber, Fig. 2, can be superposed on a true "primary" creep resulting from some microstructural modifications inside the fibers. The interpretation of the first part of the curve is not straightforward. In the same way the calculation of the true applied stress in the permanent regime of the creep test suffers from the imprecision in the number of fibers effectively loaded. The failure of the bundle is preceded by an increase of the deformation rate. Again it is difficult to separate the effect of a progressive failure of the fibers from a damage accumulation in the fibers by the formation of microcraks, cavities (tertiary creep)...

Bend stress relaxation test on bundles is a quick and efficient method to qualitatively sort out fibers in term of creep resistance[3]. The fibers are tied into a loop of radius R_0, heat treated and taken back to room temperature. The residual radius of curvature R_f is measured and a relaxation parameter $m = 1 - R_0/R_f$ is calculated. If the fiber remained elastic during the heat treatment then $m=1$ whereas $m<1$ if relaxation occurred. Wrong grading have however been obtained when fibers shrunk during the test, typically at large R_0. A negative deformation in a conventional creep test cannot be separated from a positive deformation by BSR tests.

Mechanical tests on bundles are simpler to perform, as the sensitivity of the load cells is less critical. They also reflect the way the fibers will be loaded in the composite. Fiber to fiber friction inside the bundle for example can permit some load transfer. But some ambiguity concerning the number of fibers effectively loaded renders the determination of the defect distribution difficult as well as the understanding of the microstructural mechanisms controlling deformation and failure. Testing single fibers clears this ambiguity.

Single fiber tests

The fiber has to be carefully extracted with gloved fingers from the bundle immersed in absolute alcohol in a flat container. The fiber is then placed on a cardboard frame, aligned on a straight line and fixed with epoxy glue. Fiber diameter is measured optically using a laser scan micrometer[+]. Fiber diameter has to be measured for each fiber tested as variation of 20% in the diameter of ceramic fibers can be easily found in the same bundle. The use of a mean diameter in the fiber section calculation would introduce a 40% error in the conversion of the load into stress. The prepared sample is fixed on the tensile machine[4], Fig. 3, and the central part of the cardboard is removed by cutting lateral slots from the holes which define the glue points and gauge length.

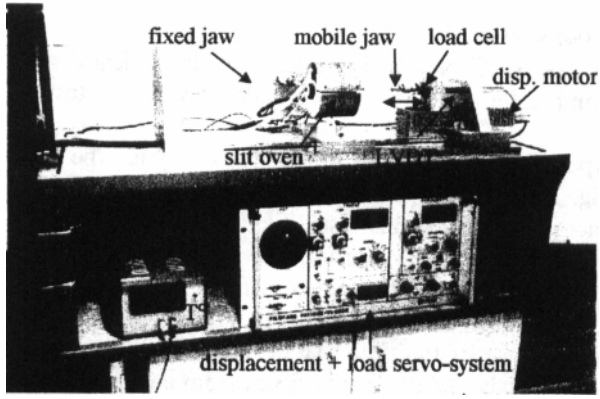

Fig. 3: High temperature tensile/creep testing machine[4]. A servo-system controls the displacement of the mobile jaw at a fixed rate for tensile test or to ensure a constant load for creep tests.

Mechanical tests on single filaments require dedicated equipment with load cell and servo system of high sensitivity of 0.1 g or better. This requirement is easily understood by considering the following example: a high temperature creep test at 250 MPa on a fiber of 10 μm in diameter, requires the servo system to maintain a constant applied load of 2 grams. A deviation of 0.5g of the servo control corresponds to a variation of 25% of the initial applied stress i.e. here 62

[+] LSM 6000 - Mitutoyo

MPa. The control of the applied load by a servo-system is preferable to applying a dead weight to the fiber, which induce an overload or a shock and can easily break the filament or perturb the primary creep recording. Direct measurement of the strain of the fibers by the laser speckle technique as been accomplished with fine ceramic fibers[5] but becomes an arduous task at high temperature. The fiber elongation is more commonly determined by measurement of ΔL_{totale}, the displacement of the mobile jaw, with a LVDT transducer Fig. 3. This requires to subtract the elongation of the experimental system Δl_{exp} (grip/glue/fiber system, load cell, frame...) for the corresponding load F, especially at small gauge lengths.

The compliance of the experimental system, $\Delta l_{exp} / F$, is determined for each new bobbin of fibers using the following equations:

$$\Delta L_{totale} / F = \Delta l_{fiber} / F + \Delta l_{exp} / F = L_0 \sigma / F.E_{fiber} + \Delta l_{exp} / F \quad (1)$$

$$\Delta L_{totale} / F = \frac{L_0}{D^2} \frac{4}{\pi E_{fiber}} + \Delta l_{exp} / F \quad (2)$$

Around twenty tensile tests are done at 4 different gauge lengths L_0, and the measured elongation per failure load $\Delta L_{Tot}/F$ is plotted as function of L_0/D^2 where D is the diameter of the single fiber tested, Fig. 4. The extrapolation of the straight line to $L_0 = 0$ gives the compliance of the experimental system $\Delta l_{exp}/F$.

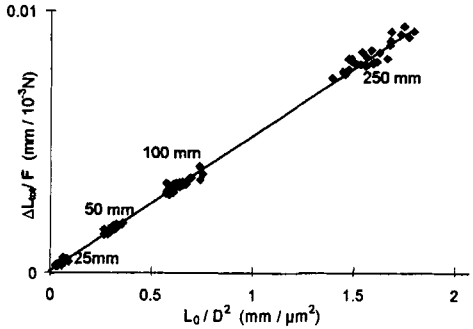

Fig. 4: The compliance of the experimental system ($\Delta l_{exp}/F$) is the Y coordinate at X=0 .

Statistical analysis of the strength distribution: Tensile tests conducted with single fibers give a straight determination of the failure stress distribution of the fibers inside the bundle, but, in order to obtain the data necessary for a statistical analysis, many test results have to be obtained. The survival probability P_S of a fiber of diameter D and length L_0 under a stress σ, can be first modelled using a unimodal Weibull distribution with a volume or a surface dependence, according to the defect location:

$$P_S(\sigma_R \geq \sigma) = \exp(-\theta_S.\sigma^m.S) \quad (3)$$

if defects are located on the fiber surface, and

$$P_S(\sigma_R \geq \sigma) = \exp(-\theta_V.\sigma^m.V) \quad (4)$$

if defects are located in the fiber volume, where σ_R is the failure stress of the fiber, m is the Weibull modulus, which characterises the width of the failure stress distribution, that is the dispersion of the size of the defects in the fiber, $\theta_S\sigma^m$ and $\theta_V\sigma^m$ are the intensity (average number per unit length) of defects associated to a failure stress lower than σ for defects located on the external fiber surface and in the fiber volume respectively. S is the external surface of the fiber tested and V its volume. The analysis of a wide range of ceramic fibers (SiC based fibers and oxide fibers) at different gauge lengths has however permitted to draw limitation that a blind utilisation of the Weibull model could give.

The use of a mean diameter in the determination of the Weibull parameters produces a significant error [6,7]. Larra-Curzio et al.[6] show that taking a mean diameter of 12μm, the m value is underestimated by a factor 1.78 if the standard deviation is of 2 μm. The fiber diameter has to be known for each fiber tested. If the variation of the diameter along one fiber can be neglected, the diameter is measured prior to each tensile test. In the case of possible variation along the gauge length, the diameter should be measured at the location of the failure. In practice this is however not always feasible as the elastic energy released during the failure makes the fiber break into several pieces and the deposition of absorbing media on the fiber surface (paraffin, grease...) is not without effect on the fiber tensile properties. In this case, the diameter profile along the gauge length is determined and the minimum diameter is taken into account.

If the fibers present variations in their diameters from one fiber to another, an effective failure stress σ_E expressed as

$$\sigma_E=\sigma_R\cdot V^{1/m} \text{ or } \sigma_E=\sigma_R S^{1/m} \qquad (5)$$

has to be introduced to reflect the effect of volume or surface variation on the failure probability. The ranking of the experimental stresses is then carried out on these effective failure stresses and the probability of failure $P_R(j)=j/(N_{Lo}+1)$ is assigned to the j^{th} fiber broken at $\sigma_{E,j}$ with $\sigma_{E,j-1} \leq \sigma_{E,j} \leq \sigma_{E,j+1}$. It can be seen that this ranking depends on the value of m which is sought. This value is estimated by an iterative calculation.

Fig. 5 shows the effective failure stress distribution of the Nextel 720 fiber from 3M[8] tested at 100mm can correctly be fitted using a unimodal Weibull law with m=6.25 and $\theta=1.15.10^4$ $GPa^{-6.25}.m^{-2}$. These parameters should permit the effective failure stress distribution at other gauge lengths to be predicted. However a systematic analysis of a large number of oxide and non oxide fibers shows that this is often not possible. A separate processing of results at another gauge length gives a distinct m value. The range of variation of these m values is larger than the expected standard deviation in the m determination for set of 30 experiments (std =0.68 for m=4 [9].) This shows that the $L_0^{1/m}$ variation of σ_E does not permit a valid description of the length effect in the fiber failures. It reflects fluctuations of the density of defects on a large scale (much larger than the gauge length), according to probable fluctuations of the physical conditions during the

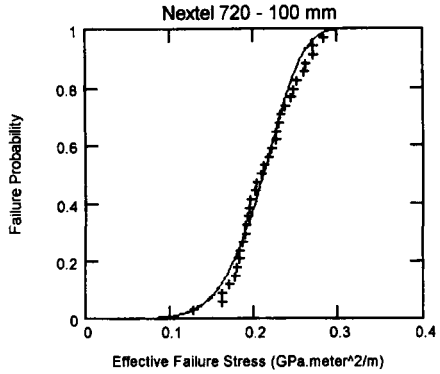

Fig. 5: The experimental failure stress distribution of Nextel 720 fiber at a gauge length of 100mm can be described with a unimodal Weibull distribution. (m=6.25 and $\theta=1.15.10^4$ $GPa^{-6.25}.m^{-2}$). An effective failure stress is used to take into account diameter variations.

elaboration of fibers. These fluctuations can be quantified by a exponent $\beta < 1$ on the length L_0 in the expression of the Weibull distribution[9]

$$P_S(\sigma_R \geq \sigma, L_0, D) = \exp\left[-\theta.\sigma^m.(L_0)^{\beta}.\left|\frac{\pi D}{\pi D^2/4}\right|\right] \quad (6)$$

The effective failure stress is then written

$$\sigma_E = \sigma_R \cdot (L_0)^{\beta/m} \left(\left|\frac{\pi D}{\pi D^2/4}\right|\right)^{1/m} \quad (7)$$

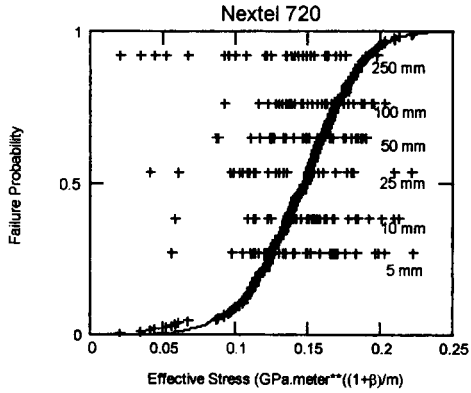

Fig. 6: The prediction of the failure probability of Nextel 720 fibers for the six gauge lengths using the same Weibull parameters (m=4.8, $\theta=6.61$ $GPa^{-4.8}.m^{-1-\beta}$) can be obtained with a power law contribution of the gauge length ($\beta=0.425$).

In Fig. 6, 180 results obtained at six gauge lengths (30 per gauge length) have been plotted on the same curve using the above formulation of the effective failure stress. The horizontal lines correspond to the repartition of the effective failure stresses. Every point of the experimental failure probability curve is vertically aligned with a cross of one of the horizontal lines corresponding to the experimental gauge length used for this point. For example the first point has been obtained at 250 mm. This experimental curve can be fitted with the distribution law of equation (6) with the three parameters m=4.8, $\theta=6.61.10^3$, $\beta=0.425$, and surface defects. The length effect is now correctly represented as the contribution of the 6 gauge lengths over the curve are similar. In the example shown, the fluctuations of the density of defects on a large scale originate from contacts with neighboring fibers in the bundle inducing their "welding" during sintering[10]. Failure distribution is then related to the interfilament distance distribution during processing, which can fluctuate at a large scale.

High temperature mechanical tests. Tests conducted in air up to 1550°C can been carried out with a tubular furnace with a lanthanum chromite heating element with an alumina inner tube, Fig. 3. The furnace is designed with a fine slot and can be slid when hot around the mounted fiber so that the very quick heating times are possible. This is especially important for high temperature tensile tests as it permits a large number of tests per hour. The load cell has to be protected from thermal radiation to avoid any drift, especially for long creep test. The jaws in this configuration remain outside the oven. Hot jaws would make the interpretation of the creep test more straightforward, but in practice reaction between the cement used to glue the fiber to the hot jaw causes a lot of failure or sliding in the grips, and increases significantly the test time.

The deformation in creep are deduced from the elongation measured by an iterative method, knowing the temperature profile along the fiber and the creep rates previously determined at lower temperatures for the same applied stress. Mathematical modeling to extract the deformation rate of a fiber subject to a temperature gradient have also been proposed[11].They can be successfully used if the activation energy for creep does not vary as the function of temperature. Silicon carbide based fibers can be tested up to 1400°C using flowing argon to reduce oxygen from the hot zone. A thin layer of silica is formed, which does not affect noticeably the creep rates. Above 1400°C this configuration has however shown its limit and closed chambers with controlled atmosphere have to be used. They have the drawback to increase dramatically the duration of the tests and a lot of care has to be put in the protection of the load cell from small temperature variations.

Microstructural observations

SEM: The defect responsible for the fiber failure is located using SEM. The broken fiber is gripped between two pieces of carbon tape. Only half a millimeter below the failure surface is kept out of the tape to avoid vibration during

observation. SEM equipped with a field emission gun can be used with an acceleration voltage of a few keV in order to avoid carbon coating of non-conductive fibers. The defect is not always identifiable, but can be often located as the center of a mirror zone of the primary fracture surface. Most often the strength controlling flaws correspond to process scratch on the surface or larger grain boundary reaching the surface or, more rarely, internal voids due to a local heterogeneity in the precursor.

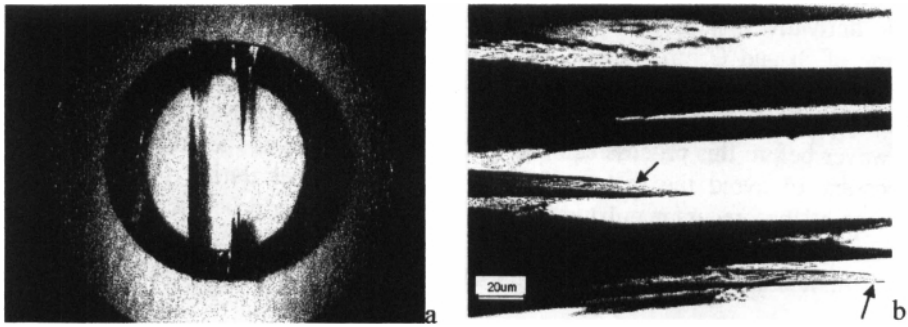

Fig. 7: Thin foil of SiC based fibers; longitudinal sections. Both the core and the surface (arrowed) can be observed in TEM[14].

TEM: The evolution of the microstructure after high temperature deformation is followed using TEM. Several methods to prepare thin (50-100 nm) foils out of ceramic fibers have been proposed. Ultramicrotomy, used for carbon fiber, has been adapted to ceramic fibers[12] , but their brittleness make them to fall into pieces under the diamond knife. Transverse section are obtained[13] by the infiltration of a bundle with epoxy followed by a mechanical thinning down to 5 μm using a wedge polishing device tripod and finally ion etched for a 15 to 60 minutes. A simple and rapid method[14] to obtain longitudinal sections is to glue a single layer of fibers on a 3 mm molybdenum ring, Fig. 7a, and to ion etched for 4 to 10 hours depending on the fiber type. The fibers must touch each other so that their surface in contact is protected from ion beam by the adjacent fibers. In this way it is possible to observe fiber from the surface to the core Fig. 7b, Fig. 14a). Modifications of the microstructure are observed in the load axis direction on such transversal sections.

SILICON CARBIDE BASED FIBERS

The strong covalent bonds between the carbon and silicon atoms in silicon carbide lead to low diffusivity and dislocation mobility within the material with the consequence that it resists grain growth and deformation and possesses a high melting point. Up to 1500°C, SiC forms an outer silica layer which slows the diffusion of oxygen into the ceramic resulting in parabolic kinetics of oxidation. The drawback of this low diffusivity is that sintering of pure stoichiometric SiC requires very high temperature and/or pressure. This difficulty can be

circumvented by the use of sintering aids but these in turn then determine and adversely affect creep behavior. The first generation of silicon carbide fibers contained only 55%wt of β-SiC grains and subsequent generations have seen the composition evolve towards stoichiometry.

Fabrication of silicon carbide based fibers

Fine diameter SiC fibers are made from precursor fibers, which are spun from the melt of an organosilicon polymer, such as polycarbosilanes (PCS) or one of their derivatives. This family of polymers is principally formed of rings of 6 atoms of Si and C, prefiguring the architecture of the blende structure of SiC. Methyl groups and hydrogen atoms are grafted onto these rings and in part remain in the fibers after their conversion to ceramic fibers by pyrolysis above 1200°C. However before this process can take place, cross-linking of the precursor fiber is necessary to avoid the softening or melting of the fiber during pyrolysis. The choices of the precursor polymers and of the cross-linking processes have a great influence on the final composition and microstructure of the ceramic fibers. A better understanding of this has led to improved SiC fiber properties.

Fibers cured by oxidation

The first fine SiC based fibers the Nicalon fibers[15] were produced from a PCS fiber for which cross-linking was achieved by a heat treatment in air at around 200°C. Lateral Si-H and C-H bonds were oxidised and Si-O-Si or Si-O-C new bonds were created linking pairs of polymer chains. This simple and cost-effective curing process had the drawback of introducing oxygen into the structure of the precursor fiber which already had hydrogen and methyl side groups in addition to the Si-C of the main chain. This deviation from stoichiometry was reduced during the heat treatment due to the outgassing of hydrogen, carbon oxides and alkyls between 300 and 900°C. However, after the pyrolysis at around 1200°C, significant amounts of oxygen (12%wt) and excess carbon (C_{at}/Si_{at} = 1.3) still remained in the ceramic.

The fibers were described as SiC based fibers, although their appearance and mechanical properties were not those which could be expected from SiC. The NL-200 Nicalon fibers, which are the most representative of this class of ceramic fibers, have a diameter of 14 μm, a glassy appearance, a Young's modulus of 200 GPa, which is half that of bulk SiC and show much inferior creep properties as creep is observed from 900°C. This is explained by the microstructure of the fiber, Fig. 8. Only 55% of the fiber is composed of β-SiC. Oxygen introduced during curing forms with carbon and silicon a metastable Si-C-O phase representing 35 to 40% of the fiber by weight, the rest of the fiber consisting of free carbon particles[16].

The Si-C-O phase lowers the ratio of atoms available to form β-SiC grains, impedes their growth and permits creep. This phase begins to decompose from 1200°C and permits a significant growth of SiC grains from 1400°C in air. Excess carbon and oxygen are lost in the form of oxides of carbon but no densification of

the remaining growing SiC grains is possible so that the fiber loses all strength. This degradation of the fiber is more rapid in an inert atmosphere than in air as the outer silica layer which is formed by oxidation slows down the outgassing of the decomposition. However voids filled with CO which build up at the SiC/SiO_2 interface reduce the fiber strength.

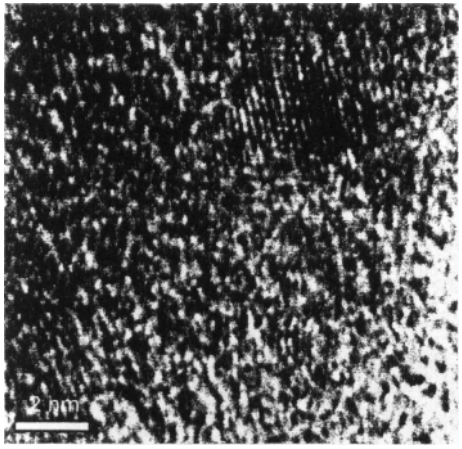

Fig. 8: The NL 200 Nicalon fiber is poorly crystallized with SiC grains of 2 nm and free carbon aggregates of 1 nm embedded into a metastable Si-C-O phase.

Ube Industries produced a series of fibers from a polytitanocarobosilane (PTC) precursor which was obtained by the grafting of titanium alkoxide between the PCS chains[17]. PTC was reported to be more easily spinnable. Tyranno LOX-M fibers with diameters down to 8.5μm and containing 13% oxygen by weight were produced after oxidation curing and pyrolysis at around 1300°C. Moreover it was expected that the germination and growth of evenly distributed small grains of TiC could trap excess carbon and inhibit the SiC grain growth responsible for the strength loss. Growth of large TiC particles was observed from 1200°C[18], but no remarkable improvements in the microstructural stability and mechanical properties were noticed and higher oxidation rates were reported.

Fibers cured by irradiation

The further improvement of SiC based fibers required the elimination of oxygen from the structure. This was achieved by Nippon Carbon by irradiating precursor PCS fibers with a 2 MeV electron beam. Si and C atom sited radicals were formed and radical-radical recombination reactions permited the chains to be crosslinked without introduction of oxygen. The fibers were pyrolysed up to about 1400°C and commercialised under the name of Hi-Nicalon[19]. The oxygen content was decreased to 0.5%wt but the fiber contained more free carbon ($C_{at}/Si_{at} = 1.39$) as less oxides of carbon could leave the fiber during heat treatment. The short duration of the pyrolysis has the effect of preventing a significant part of the Si - C from crystallising. The fiber encloses ovoid β-SiC grains of 5 to 20 nm surrounded by poorly organised Si-C and turbostratic free carbon, as seen in Fig. 9. The lower oxygen content induced a better chemical stability at high

temperature compared to oxygen cured fibers. The threshold temperature for creep was pushed to 1100°C and lower creep rates were measured. Creep resistance could further be enhanced by a post heat-treatment for 5 hours in argon at 1450°C, a temperature just above the pyrolysis temperature, so as to increase the crystallinity. The SiC grains have grown to a mean size of 30nm, some of them develop facets and come into contact with adjacent SiC grains which limits grain sliding. Turbostratic carbon layers grow preferentially parallel to some of these facets and could in some cases form cages around SiC grains limiting their growth. Longer duration of post heat-treatments or higher heat-treatment temperatures, so as to further increase the SiC grain packing, were detrimental for fiber strength and survival times in creep[18].

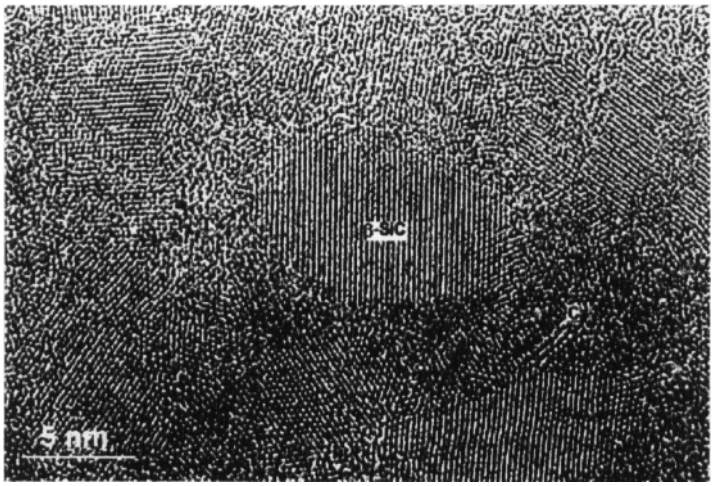

Fig. 9: Microstructure of the Hi-Nicalonf fiber exhibiting ovoid β-SiC grains of 5 to 20 nm, turbostratic carbon in a poorly ordered Si-C phase.

The radiation curing process was also used by Ube Industries to cross-link PTC fibers: after a pyrolysis at around 1300°C the LOX-E fiber contained 5% wt of oxygen. This higher value of oxygen compared to that of the Hi-Nicalon was due to the introduction of titanium alkoxides for the fabrication of the PTC. As a result, the LOX-E fiber possessed a microstructure and high temperature behavior which were comparable to those of the previous oxygen rich fibers[18]. A subsequent series of Tyranno fibers was obtained from a PCS polymer onto which zirconium acetylacetonate was grafted[20]. Compared to titanium alkoxides these compounds introduced less oxygen and permited the oxygen content to be decreased to 2%wt. The microstructure and creep behavior of the Tyranno ZE fibers obtained by radiation curing were close to that of the Hi-Nicalon.

Sintered fibers

If significant improvements were brought about by the use of radiation curing compared to oxidation curing, the microstructures and creep behaviors obtained were not those of sintered silicon carbide. Attempts to attain such microstructures by post heat-treatment led to increasingly brittle fibers. Moreover the fibers contained a significant amount of free carbon which could help control the SiC grain growth but increased the sensitivity of the fiber to oxidation. Sintered fibers could only be obtained by a modification of the fabrication processes.

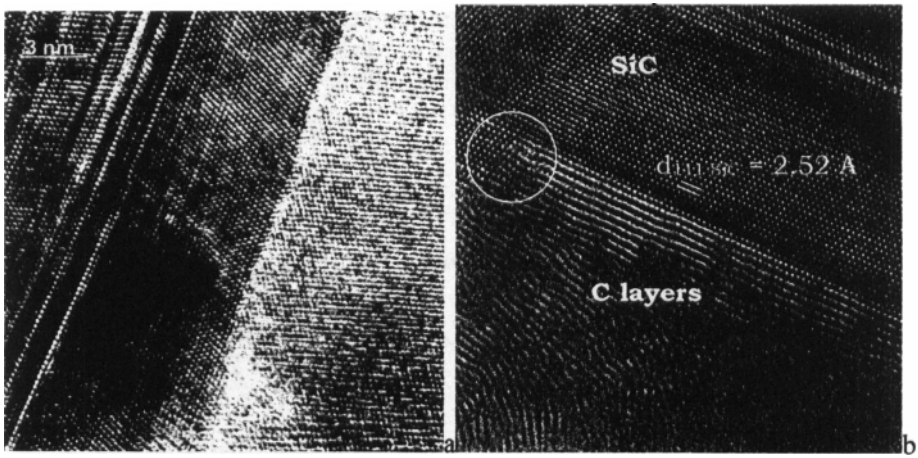

Fig. 10: Typical intergranular structures in sintered SiC fibers: a) clean SiC/SiC grain boundary close to Σ9. facets. b) Graphen layers in epitaxy with (111) SiC planes. Hi-Nicalon Type S fibers.

Ube Industries, (Tyranno SA[21]), and Dow Corning (Sylramic[22]) start with precursor fibers cured by oxidation, as for the first generation of fibers, but introduce sintering aids in the precursor, by reaction of aluminium acetylacetonate with PCS for Ube Industries or by doping the PTC with boron for Dow Corning. By these processes ceramic fibers containing an oxygen rich intergranular phase, similar to the first generation of fibers, are produced. These fibers are then pyrolysed up to 1600°C for the Sylramic and 1800°C for the Tyranno SA, so that the excess carbon and oxygen can be lost as volatile species. Unlike in the previous generations of fibers, densification of the fibers can take place through sintering aids. Grain sizes are of 200nm, with TiB_2 particles in the Sylramic fibers whereas no crystallised aluminium compounds are formed in the Tyranno SA fibers. The process adopted by Nippon Carbon (Hi-Nicalon Type S[23]) is reported as being a "modified Hi-Nicalon process". The PCS precursor fibers are cured by irradiation and pyrolysed in a hydrogen rich atmosphere up to 1500°C to reduce the free carbon content. The grain sizes are 50 to 100nm. Sintering aids could not be detected in these fibers. The three types of fibers have clean SiC/SiC boundaries, Fig. 10a), but contain a significant amount of free carbon located at pockets between clusters of SiC grains which explains why their Young's moduli

are still lower that that of bulk sintered SiC (Tyranno SA: E=330 GPa, Type S: E=375 GPa, Sylramic E=390 GPa). Epitaxial growth of C graphen planes on SiC (111) have been revealed,which inhibits SiC grain growth Fig. 10b).

The three fibers show much improved creep properties [24,25] with creep rates of the order of $10^{-8}sec^{-1}$ at 1400°C. The Nicalon Type S fiber shows lower creep rates than the other two fibers Fig. 11 and this fiber is also seen to maintain its room temperature strength up to 1400°C. The use of the electron curing process for the PCS precursor is clearly of benefit although it imposes a cost penalty. The sintering aids used in the other two fibers are seen to increase creep rates by increasing diffusion rates. Moreover internal decomposition of silicon carbide into SiO and free carbon has been seen in the cores of the Sylramic fibers and the first generation of Tyranno SA1 fibers (Fig. 13) due to some residual oxygen. This led to premature failure compared to Hi-Nicalon Type S fibers. The elimination of oxygen in following versions of Tyranno fibers SA has been better achieved.

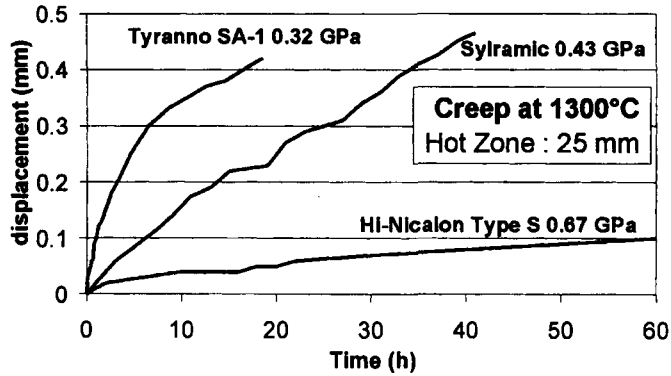

Fig. 11 Creep curve obtained at 1300°C for three near-stoichiometric SiC fibers

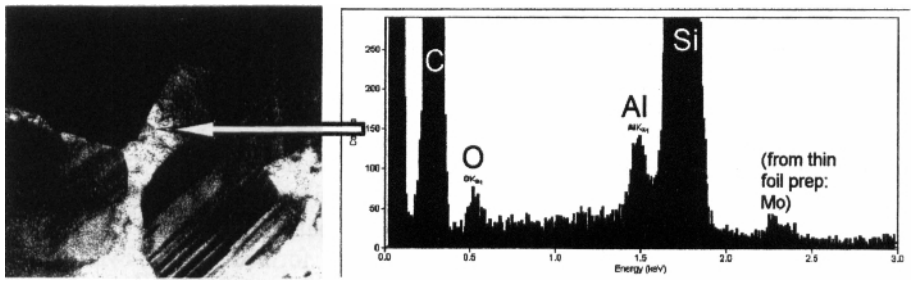

Fig. 12 : EDX analysis of the intergranular carbon rich region in the core of Tyranno SA1 fiber showing the presence of oxygen and aluminum.

As the composition of the fibers approaches stoichiometry, lower creep and oxidation rates are obtained. Nevertheless compared to bulk SiC the development of a micrometer size oxide layer has a greater effect on the properties of the

composites. CMCs rely for their tenacity on their ability to accumulate cracks. These cracks are however paths for diffusion of oxygen. Silica layers created on the fibers in the vicinity of cracks fuse the fibers to the matrix seriously reducing fiber pull-out and the absorption of failure energy of the composite. For this reason, this family of fibers are likely to be limited to a maximum temperature of 1400°C, unless complex coatings or self healing matrices could prevent their oxidation.

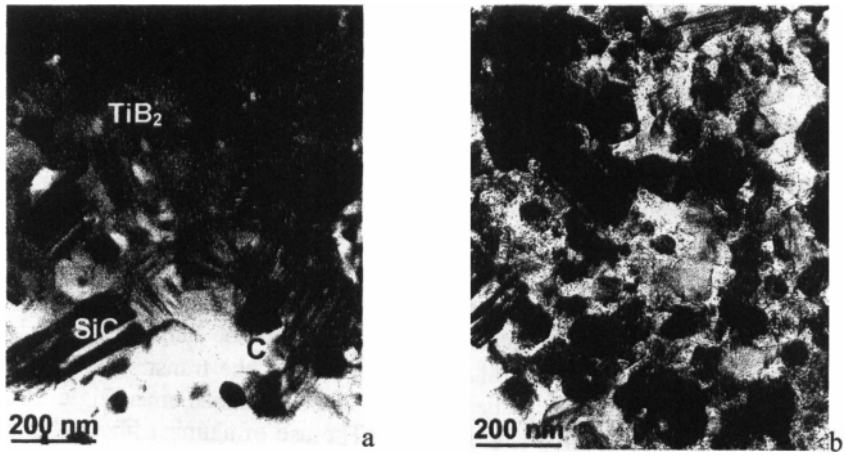

Fig. 13 : Sylramic fiber : a) as received and b) after creep at 1300 °C, 400 MPa for 12 hours. SiC grains in the center of the fiber are decomposed into SiO and C.

OTHER NON OXIDE FIBERS

Various non oxide fibers have been developed at a laboratory or pilot scale from other silicon containing precursors such as polysilazane. The fibers obtained have amorphous structures based on Si-C-N-O, Si-N or Si-B-N-C but recrystallise from 1200°C or show poor oxidation resistance. Boron Nitride fibers with oriented turbostratic structures are also being developed for specific applications but they are intrinsically not adapted to resist oxidation.

ALUMINA-BASED FIBERS

If high performance fibers are to be exposed to oxidative atmospheres and temperatures above 1400°C, they will have to be made from oxides with high melting points. Alpha-alumina is widely used for it refractory properties. Its complex structure provides large Burgers vectors so that high stresses are necessary to generate plasticity in monocrystals. Monocrystalline α-alumina fibers showing no creep up to 1600°C can be obtained if the fiber axis strictly corresponds to the [0001] axis. However no viable processes exist at present to produce fine and flexible continuous monocrystalline fibers. Therefore only polycrystalline fibers can be considered for the reinforcement of ceramic

structures. Various processing routes exist for making such fibers and these lead to a large range of microstructures and behaviors at high temperature.

Precursors of alumina are viscous aqueous solutions of basic aluminium salts, $Al\ X_n\ (OH)_{3-n}$, where X can be an inorganic ligand (Cl^-, NO^{3-}...) or an organic ligand ($HCOOH^-$...)[26]. Spinning of the precursor produces a gel fiber which is then dried and heat treated. Decomposition of the precursor induces the precipitation of aluminum hydroxides, such as boehmite AlO(OH), and the outgassing of a large volume of residual compounds. The associated volume change and porosity at this step has to be carefully controlled. It is also possible to directly spin aqueous sols based on aluminum hydroxides. Dehydration between 300°C and 400°C yields amorphous aluminas and leaves nanometer size pores in its structure. Heating up to around 1100°C induces the sequential development of transitional forms of alumina. These aluminas have spinnel structures containing aluminum vacancies on the octahedral and tetrahedral sites. They only differ by the degree of order in the distribution of these vacancies. At this stage the fiber is composed of alumina grains of a few tens of nanometers, poorly sintered with a finely divided porosity. Above 1100°C stable α-alumina nucleates and a rapid growth of micron sized grains occurs together with coalescence of pores. Porosity generated during the first steps of the formation of metastable aluminas cannot be eliminated and is increased by the higher density of α-alumina compared to the transitional forms. The fibers become extremely brittle due to large grain boundaries emerging at the fibers' surfaces and cannot be used in this form. The use of alumina fibers above 1100°C requires the control of the nucleation and growth of α-alumina and porosity. This is has been achieved by adding either silica precursors or seeds for α-alumina formation to the fiber precursors and has led to two classes of alumina based fibers.

Alumina-Silica fibers

Alumina-silica fibers were the first ceramic fibers produced in the early 1970s, for thermal insulation applications. A small amount of silica (≈3 % wt in the Saffil short fibers from ICI) permits the sintering of the transitional forms of alumina and delays the nucleation and growth of α-alumina to 1300°C[27]. Larger amounts (15%wt in the Altex fiber from Sumitomo) produce γ-alumina grains of around 25nm in amorphous silica[28]. Mullite, with a composition between $2Al_2O_3.SiO_2$ and $3Al_2O_3.2SiO_2$, crystallises above 1100°C, before the formation α-alumina, the growth of which is then restricted. The α-alumina formation can be totally suppressed if enough silica is added to consume the metastable alumina by mullite formation. Boria has been added to the 3:2 mullite composition by 3M to lower the temperature of mullite formation, help sintering and increased the fiber strength. Various degrees of crystallinity can be obtained according to the amount of boria and the pyrolysis temperature[29,30]. However the high temperature resistance which could be expected from the complex mullite structure is not obtained due to the presence of an amorphous boro-silicate intergranular phase.